

## FLUOROMETRIC DETERMINATION OF HYDROGEN PEROXIDE USING $\text{Fe}_3\text{O}_4$ MAGNETIC NANOPARTICLES AS A MIMETIC ENZYME

X. FENG<sup>a,b</sup>, J. YANG<sup>b</sup>, S. WU<sup>b</sup>, D. LIAO<sup>a,\*</sup>

<sup>a</sup>*School of Chemistry and Chemical Engineering, Guangxi University, Nanning, Guangxi 530004, China*

<sup>b</sup>*Medical College, Guangxi University of Science and Technology, Liuzhou, Guangxi, 545006, China*

Hydrogen peroxide ( $\text{H}_2\text{O}_2$ ) is used as a chemical in many food industries and excessive residual  $\text{H}_2\text{O}_2$  in the food will cause harm to people's health. To establish a simple, low-cost and accurate analytical methods to detect  $\text{H}_2\text{O}_2$  by using metal oxide nanoparticle as mimetic enzyme. In this paper, we utilized the instinct peroxidase-like property of  $\text{Fe}_3\text{O}_4$  magnetic nanoparticles ( $\text{Fe}_3\text{O}_4\text{MNPs}$ ) to establish a fluorescence assays of  $\text{H}_2\text{O}_2$  and benzoic acid (BA) as indicator.  $\text{Fe}_3\text{O}_4\text{MNPs}$  were prepared by co-precipitation and characterized using TEM, magnetization and  $\text{N}_2$ -BET surface area measurement. The fluorescence of system (with excitation/emission peaking at 294/411 nm) was enhanced on increasing the concentration of  $\text{H}_2\text{O}_2$  due to form hydroxybenzoic acid. Under optimized conditions, the system gave a ratiometric fluorometric response in the 0.5 to 12.5  $\mu\text{M}$   $\text{H}_2\text{O}_2$  with a 0.122  $\mu\text{M}$  limit of detection. The  $E_a$  and  $K_m$  for the reaction of  $\text{H}_2\text{O}_2$  with the  $\text{Fe}_3\text{O}_4\text{MNPs}$  were respectively calculated to be 44.65 kJ/mol and 234.30 mM. The system is highly sensitive and selective toward  $\text{H}_2\text{O}_2$  which the relative standard deviation (RSD) of samples was 4.86% ( $n=6$ ). The proposed method provides a quick, easy and cheap way and was applied to the determination of  $\text{H}_2\text{O}_2$  in disposable chopsticks with satisfactory results. The average hydrogen peroxide content in disposable chopsticks was  $2.321 \pm 0.32$  mg/kg. The method for  $\text{H}_2\text{O}_2$  determination described here would be of great value in food and agricultural industry.

(Received April 13, 2020; Accepted September 18, 2020)

*Keywords:* Hydrogen peroxide,  $\text{Fe}_3\text{O}_4$  magnetic nanoparticles, Mimetic enzyme, Fluorescent spectrometry

### 1. Introduction

Hydrogen peroxide ( $\text{H}_2\text{O}_2$ ) is a very important chemical in environmental and biological studies and it is also used as a chemical in many food industries. These include uses in the meat processing, cleaning product and dairy industry[1]. Hydrogen peroxide is a major food bactericide which was used to prevent microbial proliferation on fish products, noodles, soybean products and so on[2,3]. Also dining utensils, especially the disposable chopsticks made of

---

\* Corresponding author: liaodankuigx@163.com

bamboo, are often treated with  $H_2O_2$  for bleaching and sterilization [4]. Accidental food poisoning was caused by excessive amounts of residual hydrogen peroxide in processed foods which were treated by  $H_2O_2$ , such as udon and noodles [5]. Excessive residual  $H_2O_2$  in the food will cause harm to people's health. A growing concern about residual  $H_2O_2$  in foods and other items used in daily life has caught everyone's concern. It is important to detect the concentration of hydrogen peroxide.

Until now, several methods have been investigated to detect  $H_2O_2$ , including spectrophotometry[6-9], fluorometry[10-12], chemiluminescence[13,14] and electrochemistry[15,16]. Among these techniques, the horseradish peroxidase (HRP) catalyzed reaction is one of the most widely used in  $H_2O_2$  detection. But these enzymatic reaction on its natural enzyme had also some limitations, such as easy denaturation, high price and time consuming. As highly stable and low-cost alternatives to natural enzymes, artificial enzymes have aroused widely concern and it is pushed forward by substituting natural enzyme with novel artificial enzymes, such as  $Fe_3O_4$  nanoparticles [17]. Chang used  $GOx/Fe_3O_4/GO$  nanoparticles as a catalyst to detect  $H_2O_2$  and glucose with  $N,N$ -diethyl- $p$ -phenylenediamine as substrate by colorimetry [18]. Xu used  $Hb/Fe_3O_4/Au$  nanoparticles as a catalyst to detect  $H_2O_2$  by electrochemistry[19]. Although, these  $Fe_3O_4$ MNPs complexes have exhibit unexpected horseradish peroxidase activity, large surface-to-volume ratio and highly stability. The preparation of nanostructured materials is relatively difficult. Based on alternatives to HRP, various sensitive fluorometric methods have been developed for the  $H_2O_2$  determination[20,21]. Luo used the multiferroic  $BiFeO_3$  as peroxidase mimetic catalyst to detect  $H_2O_2$  on  $BiFeO_3 / H_2O_2/BA$  system which exhibited high sensitivity and low detection limit [22]. Despite their success in various applications, there are still some concerns related to the use of these aforementioned catalysts, either low catalytic activity or difficult synthesis. Thus, it is necessary to establish a simple, low-cost and accurate analytical methods to detect  $H_2O_2$ .

Benzoic acid is a naturalistic organic acid which is cheap and easy to get. In this study, we developed a general  $H_2O_2$ -involved fluorescence system using  $Fe_3O_4$ MNPs as peroxidase mimetic enzyme and benzoic acid (BA) as indicator. The weakly fluorescent benzoic acid (BA) can be oxidized by  $Fe_3O_4$ MNPs as peroxidase mimetic enzyme to form strong fluorescent hydroxyl benzoic acid in the presence of  $H_2O_2$  [23]. The fluorescence intensity of the product hydroxyl benzoic acid (Ex 294 nm, Em411 nm) was found to be proportional to the concentration of  $H_2O_2$ . Therefore, a simple, low-cost and accurate fluorometric method for the determination of  $H_2O_2$  was developed on the basis of the  $Fe_3O_4$ MNPs. Moreover, the  $Fe_3O_4$ MNPs only took one step to prepare, the reagents used in this method are simple, and the operation procedures for the analysis are very easy. The proposed technique was successfully applied to the determination of  $H_2O_2$  in disposable chopsticks.

## 2. Materials and methods

### 2.1. Chemicals and reagents

Hydrogen peroxide (30%) was purchased from Kelon Chemical Reagent Factory (Chengdu, China) and diluted to 10:1 which was calibrated by permanganate titration. The working solutions were diluted to certain percentage before used.

Benzoic acid (99%) was purchased from Damao Chemical Reagents Company (Tianjin, China). Ferric chloride, ferrous chloride, hydrochloric acid, sodium hydroxide, sodium bicarbonate were obtained from Aladdin Reagent Company. All chemicals used were of analytical reagent grade without further purification. All solutions were prepared with ultrapure water ( $> 18\text{M}\Omega\text{ cm}$ ) obtained from a Millipore Milli-Q water purification system.

## 2.2. Apparatus

The fluorescence (FL) measurements were carried out on a fluorescence spectrophotometer RF-5301 PC (Shimadzu, Japan). The Fourier transform infrared (FT-IR) spectra were acquired on the Nicolet 6700 FT-IR spectrometer (Thermo, America). The nanoparticle size were measured by Laser Particle Size Analyzer Nano S90 (Malvern, England) and dried by vacuum freeze dryer FD-1A-50 (Beijing Laboratory equipment co. LTD, China). The morphology study of the nanoparticles were done using JEM-2100 transmission electron microscopy (JEOL, Japan). Specific surface area, pore size distribution, and pore volume measurements were performed using a Micromeritics ASAP 2420-4 gas adsorption analyzer. Magnetic hysteresis loop was measured with superconducting quantum interference device (SQUID) magnetometer PPMS-9T-DynaCool (Quantum Design, USA).

## 2.3. Synthesis of $\text{Fe}_3\text{O}_4$ magnetic nanoparticles

$\text{Fe}_3\text{O}_4$ MNPs were synthesized according to the coprecipitation method [24]. Briefly,  $\text{FeCl}_3 \cdot 6\text{H}_2\text{O}$  and  $\text{FeCl}_2 \cdot 4\text{H}_2\text{O}$  in a molar ratio of 2:1 were dissolved in 100 mL purified water followed by the addition of moderate 25%  $\text{NH}_3 \cdot \text{H}_2\text{O}$  (v/v) slowly. The mixture was stirred vigorously in 30°C water bath under nitrogen protection for 30 min, then heated at 80°C for 30 min. The products were separated using the magnet and further washed several times with ethanol and purified water and then kept in ethanol.

## 2.4. $\text{H}_2\text{O}_2$ detection with the $\text{Fe}_3\text{O}_4$ magnetic nanoparticles

According to previous reports [23] with minor modifications, the experiments of fluorescence detection of  $\text{H}_2\text{O}_2$  with  $\text{Fe}_3\text{O}_4$ MNPs as catalysts were performed as follows: 0.5 mL BA (1 mM), 1 mL  $\text{Fe}_3\text{O}_4$ MNPs (1 mg/mL), 3.45 mL glycine - hydrochloric acid buffer (50 mM, pH 3.0) and 50  $\mu\text{L}$  given concentration of  $\text{H}_2\text{O}_2$  were added into calibrated test tube, sequentially. The mixture was incubated at room temperature for 30 min and added 0.2 M NaOH solution to terminate the reaction. The mixture were separated by magnet and the fluorescence spectra (with excitation/emission peaking at 294/411 nm) of supernate were recorded on a spectrofluorometer with a quartz cell (1 cm  $\times$  1 cm cross-section) and the bandwidths for both excitation and emission were set to 5 nm. Meanwhile, to acquire the optimum reaction condition, the influence of reaction temperature, reaction time, reaction pH, the concentration of  $\text{Fe}_3\text{O}_4$ MNPs and BA on the fluorescence intensity were researched. Moreover, the optimal reaction conditions for the  $\text{Fe}_3\text{O}_4$  / $\text{H}_2\text{O}_2$ /BA system were used for the determination of  $\text{H}_2\text{O}_2$  at different concentrations (0.5-12.5  $\mu\text{M}$ ) according to the procedure above. The fluorescence intensity of blank solution was measured under the same conditions. This experiment was repeated three times, and the average fluorescence signal was obtained.

### 2.5. Thermodynamic and kinetic analysis of Fe<sub>3</sub>O<sub>4</sub>MNPs as nanoenzyme

The catalytic decomposition of H<sub>2</sub>O<sub>2</sub> by the Fe<sub>3</sub>O<sub>4</sub>MNPs was studied at different temperatures. The activation energy ( $E_a$ ) was calculated using the Arrhenius equation (Eq. 1):

$$\ln k = -\frac{E_a}{RT} + \ln A \quad (1)$$

The steady-state kinetic assays were carried out at room temperature in 3.45 mL of glycine - hydrochloric acid buffer (50 mM, pH 3.0) with 1 mL Fe<sub>3</sub>O<sub>4</sub>MNPs (1 mg/mL) in the presence of H<sub>2</sub>O<sub>2</sub> and BA. The kinetic analysis of Fe<sub>3</sub>O<sub>4</sub>MNPs with H<sub>2</sub>O<sub>2</sub> as the substrate was performed by varying the concentrations of H<sub>2</sub>O<sub>2</sub>. The fluorescence intensities were monitored at a 411 nm emission wavelength every 60 s during the first 5 min by the RF-5301 PC spectrofluorometer. The reaction rates were then obtained by calculating the slopes of initial fluorescence intensity changes with time. Catalytic parameters were determined by fitting data to the Michaelis–Menten equation (Eq. 2):

$$V = \frac{V_{\max}[S]}{K_m + [S]} \quad (2)$$

### 2.6. Measurement of Residual H<sub>2</sub>O<sub>2</sub> in Chopsticks

Nine samples of disposable chopsticks were obtained from restaurants of three universities in China. These samples were cut into small pieces about 0.1 cm length and extracted with purified water [10 mg per mL of water (w/v)] at 4 °C for 24 h according to modified literature procedures [24]. The solutions were then centrifuged at 20000 r/min for 5 min at 4 °C. The eluent was assayed using the fluorescence method described above. Blank solutions were prepared by mixing 100 μL of the water in the reaction system. The fluorescence intensity at 411 nm was recorded.

## 3. Results and discussion

### 3.1. Characterization of the magnetic nanoparticles

Fig. 1a showed that the mean diameter was determined to be approximately 15 nm and the synthesized Fe<sub>3</sub>O<sub>4</sub> nanoparticles were distributed uniformly and spheres are interconnected with each other. The maximum magnetization value was evaluated by plotting magnetization (M) versus magnetic field (H) (Fig. 1b). The hysteresis loops passed through the original point and the Fe<sub>3</sub>O<sub>4</sub>MNPs was superparamagnetism. Saturation loop measurements showed that saturation magnetization is 63.33 emu/g at 300 K.

On the basis of the analysis of N<sub>2</sub> sorption measurement, Brunauer-Emmett-Teller (BET) measurements of the particle surface areas gave values of 73.91 m<sup>2</sup>/g which is higher than the others [25]. As shown in Fig. 1c, the N<sub>2</sub> absorption-desorption isotherm is close to a combination form of type II and type III according to the IUPAC classification. From Fig. 1c, the corresponding BJH mesopore size distribution indicates the pore sizes are mainly between 1.71–51.2 nm and the size distribution is quite broad with a maximum at 18.01 nm. It is shown that the Fe<sub>3</sub>O<sub>4</sub>MNPs samples have mesoporous and macroporous structure.

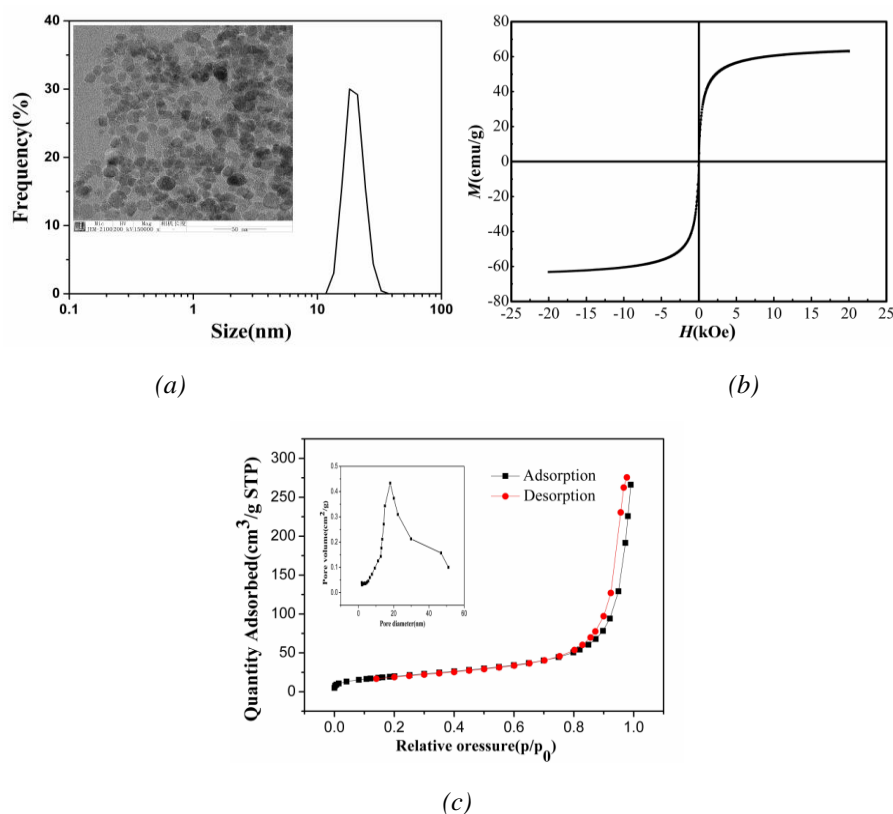


Fig. 1. (a) The morphology and size of  $\text{Fe}_3\text{O}_4$ MNPs, (b) The room temperature hysteresis loops of the  $\text{Fe}_3\text{O}_4$ MNPs and (c) Nitrogen adsorption isotherms and Pore size distributions calculated for  $\text{Fe}_3\text{O}_4$ MNPs.

### 3.2. $\text{H}_2\text{O}_2$ detection with the $\text{Fe}_3\text{O}_4$ magnetic nanoparticles

As shown in Fig. 2a, the fluorescence intensity is 22 times higher in the system of BA +  $\text{Fe}_3\text{O}_4$ MNPs +  $\text{H}_2\text{O}_2$  than that of the system of BA, BA +  $\text{Fe}_3\text{O}_4$ MNPs, BA +  $\text{H}_2\text{O}_2$  and  $\text{Fe}_3\text{O}_4$ MNPs+  $\text{H}_2\text{O}_2$ . There was a characteristic fluorescence in the system of BA +  $\text{Fe}_3\text{O}_4$ MNPs +  $\text{H}_2\text{O}_2$  at the  $E_x = 294$  nm,  $E_m = 411$  nm which is hydroxybenzoic acid. Hydrogen oxide and BA were adsorbed on the surface of  $\text{Fe}_3\text{O}_4$ MNPs. As a mimetic enzyme,  $\text{Fe}_3\text{O}_4$ MNPs catalyzed hydrogen peroxide by partial electron exchange ( $\text{Fe}^{3+}/\text{Fe}^{2+}$ ) to produce hydroxyl with strong oxidization. The benzene ring on BA was easily to be oxidized by the hydroxyl to generate hydroxyl benzoic acid with strong fluorescence by electrophilic substitution. (Fig. 2b). The reaction between BA,  $\text{Fe}_3\text{O}_4$ MNPs and  $\text{H}_2\text{O}_2$  quantitatively yields hydroxybenzoic acid immediately, allowing the selective and sensitive determination of  $\text{H}_2\text{O}_2$  by measuring the fluorescence intensity of the as-generated hydroxybenzoic acid. The substrates BA is stable, cheaper and easy to obtain. Moreover, the superparamagnetism of  $\text{Fe}_3\text{O}_4$ MNPs resulted in higher magnetic separation (<10 s). Hence, the reagents used in this method are simple, and the operation procedures for the analysis are very quick and easy.

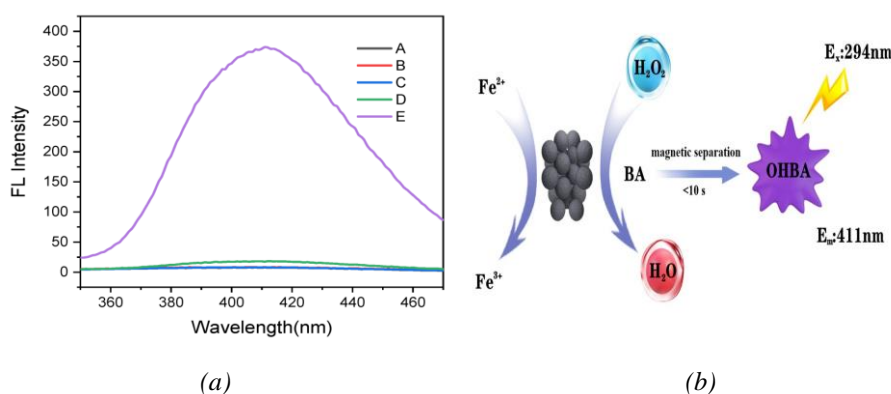


Fig. 2. (a) The fluorescence changes of system under different conditions: A:BA; B:BA+  $Fe_3O_4$ MNPs; C:  $Fe_3O_4$ MNPs +  $H_2O_2$ ; D: BA+  $H_2O_2$ ; E: BA+  $Fe_3O_4$ MNPs +  $H_2O_2$ . (b) Schematic illustration of fluorometric detection of  $H_2O_2$  catalyzed by using  $Fe_3O_4$ MNPs.

pH is one of the important factors influencing enzyme activity as the same as nanoenzyme. Fig. 3a presented the pH dependence on  $Fe_3O_4$ MNPs /  $H_2O_2$ /BA fluorescence system where a large decrease was observed from pH 3.0 to pH 5.0. The peak value was obtained at pH 3.0 and the detection condition (pH=3.0) was selected for subsequent experiments. The same nanoparticles can simulate the activity of different enzymes [26].  $Fe_3O_4$ MNPs simulate the activity of peroxidase under the acidic conditions and catalase activity under the alkaline conditions, which is consistent with previously published literature[27]. Under strong acidic conditions (PH<3.0), the formation of  $Fe^{2+}$  on the surface of  $Fe_3O_4$ MNPs may be inhibited by excessive  $H^+$  which decreased hydroxyl and reduced fluorescence intensity of hydroxyl benzoic acid.

The effect of reaction time on the  $Fe_3O_4$ /  $H_2O_2$ /BA fluorescence system were also studied. As we can see from Fig. 3b, the fluorescence intensity increases with increasing time from 10 to 40 minutes while remain stable with further increase. Considering times and working efficiency, the reaction time of subsequent experiments is 40 min.

The concentration of  $Fe_3O_4$ MNPs on the  $Fe_3O_4$ MNPs /  $H_2O_2$ /BA fluorescence system were also studied. As we can see from Fig. 3c, the fluorescence intensity increases with increasing  $Fe_3O_4$ MNPs amount from 0.05 mg/mL to 0.2 mg/mL while decreases sharply with further increase. So the concentration of  $Fe_3O_4$ MNPs of subsequent experiments is 0.2 mg/mL.

The effect of temperature on the  $Fe_3O_4$ MNPs/ $H_2O_2$ /BA fluorescence system was also studied and results are depicted in Fig. 3d. In a typical operation, before fluorescence detection, the mixture was incubated at a given temperature for 40 min. This procedure was repeated at different temperatures. As we can see from Fig. 3d, the response increases with increasing temperature from 20 to 60°C while decreases sharply with further increase in temperature which is attributed to the speed of the molecular movement increased with the temperature. As the acceleration of reaction rate, the content of hydroxyl benzoic acid increased and the fluorescence intensity increased. However, the decomposition of hydrogen peroxide will be accelerated when the temperature increase, which result in decline of fluorescence intensity. The fluorescence intensity of the system was the highest at 60°C, which was used in subsequent measurements.

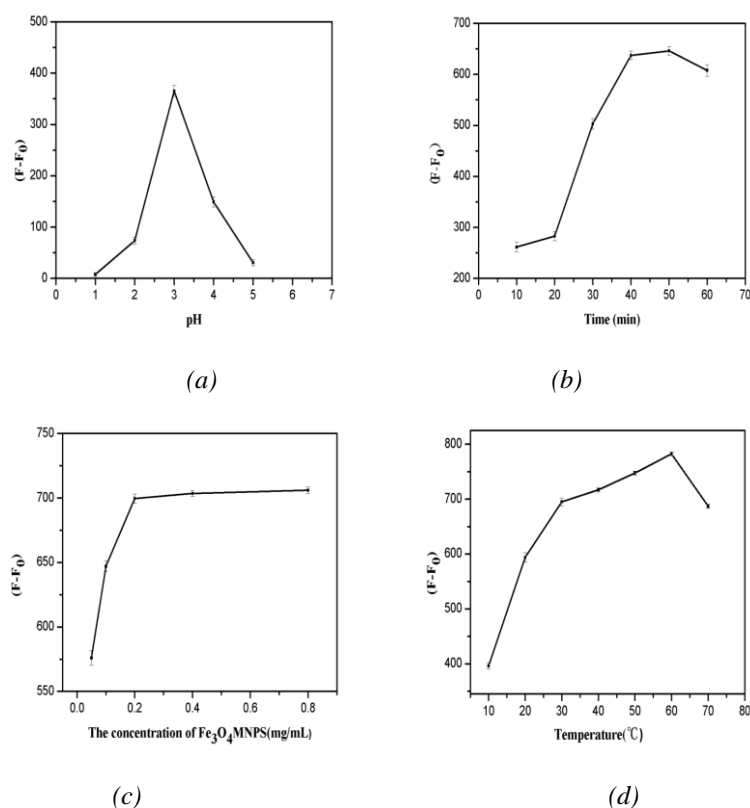


Fig. 3. Effect of (a) pH, (b) time, (c) concentration of  $Fe_3O_4$ MNPs and (d) temperature on  $Fe_3O_4$ MNPs /  $H_2O_2$ /BA fluorescence system.

### 3.3. Thermodynamic and kinetic analysis

Determination of the catalytic activity of the  $Fe_3O_4$ MNPs on fluorescence system at different temperatures not only provides the optimal ranges of temperature, but also allows estimation of  $E_a$ . The linear plots of  $\log [H_2O_2]_t$  vs time indicate that the reactions follow first order kinetics (Fig. 4a). The rate constant  $k$  can be calculated from the slope of the curves. And then the  $E_a$  for the reaction of  $H_2O_2$  with the  $Fe_3O_4$ MNPs was calculated to be 44.65 kJ/mol using the Arrhenius equation, while the  $E_a$  for thermal decomposition of  $H_2O_2$  was found to be 210 kJ/mol [28]. So the  $Fe_3O_4$ MNPs lower the energy barrier for  $H_2O_2$  decomposition, similar to the nanoenzyme. For example, the  $E_a$  for the reaction of  $H_2O_2$  with the  $Co_3O_4$ NPs was found to be 42.8 kJ/mol [29].

At the constant concentration of  $Fe_3O_4$ MNPs, the initial rates exhibit the approximative saturation kinetics with the increase of  $H_2O_2$  concentration (Fig. 4b). The Lineweaver–Burk double reciprocal plots (Fig. 4b) show the good linear relationship between  $1/v$  and  $1/[S]$ , which indicate the reaction follow the typical Michaelis–Menten model. The  $K_m$  of the reaction catalyzed by the  $Fe_3O_4$ MNPs in this study was calculated to be 234.30 mM. The  $K_m$  value of the  $Fe_3O_4$ MNPs with  $H_2O_2$  in another study of Dong *et al* was 479.91 mM [30]. Smaller  $K_m$  values demonstrate a stronger affinity between the enzyme and the substrate. The above results indicate that the presence of more “activesites” on the surface of the  $Fe_3O_4$ MNPs in this study.

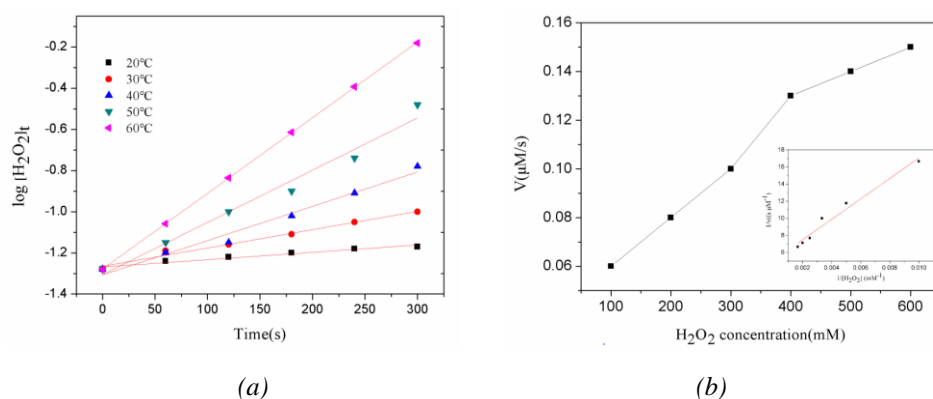


Fig. 4.(a) Kinetics of catalytic  $H_2O_2$  decomposition by the  $Fe_3O_4$  MNPs at different temperatures and (b) the Michaelis-Menten curve and Corresponding Lineweaver–Burk linearization of  $Fe_3O_4$  MNPs.

### 3.4. Standard curve of hydrogen peroxide

In this way, a fluorometric method for the determination of  $H_2O_2$  easily realized in this work. As shown in Fig. 5a, the fluorescence intensity of reaction system increases with the increase of  $H_2O_2$  concentration. Fig. 5b shows a typical  $H_2O_2$  concentration response curve, suggesting that this method has a linear range between  $0.5\mu M$  and  $12.5\mu M$ . The linear regression equations and linear region were determined using Origin data analysis software and listed as follow:  $F-F_0=55.642c+91.352$ ,  $R^2=0.993$ . Within linear region of  $0.5-12.5\mu M$ , the fitting curve showed admirable linearity, with the limit of detection (LOD) was determined to be  $0.122\mu M$  ( $S/N=3$ ).

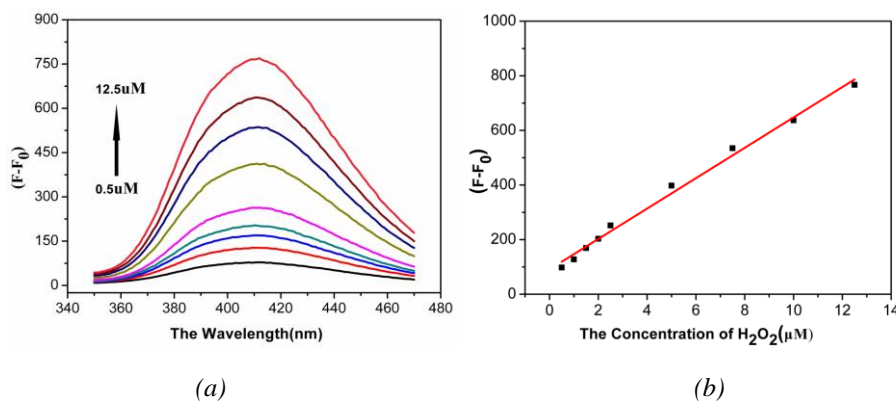


Fig. 5. (a) The fluorescence emission spectra of reaction system with the increase of  $H_2O_2$  concentration ( $0.5-12.5\mu M$ ) and Calibration curve of the  $H_2O_2$ . (b) The linear correlation between the  $\Delta F$  and  $H_2O_2$  concentration, where  $\Delta F=F-F_0=F(H_2O_2, 411nm)-F(\text{blank}, 411nm)$ . Reaction conditions:  $1.0mg/mL Fe_3O_4$  MNPs  $1mL$ ,  $1.0mmol/L$  BA  $0.5mL$ ,  $4.45mL$  pH 3.0 glycine-hydrochloric acid buffer, various concentrations  $H_2O_2$   $50\mu L$ , and reaction time 40 min.

Table 1 has summarized the analytical performances of the new methods and previously reported methods for the determination of  $H_2O_2$ . In comparison with the methods reported in the literature, among the fluorospectrophotometry methods, our work exhibited competitive

performance with relative lowest detection limit in lower concentration range. It is well-known that the surface chemisorption and catalytic activities and selectivities is varying with the size and/or shape of the catalytically active species, such as, metal nanoparticles[31]. The catalytic activity is derived from  $\text{Fe}^{2+}$  on the surface of  $\text{Fe}_3\text{O}_4$ MNPs with the particle surface areas of  $73.9140 \text{ m}^2/\text{g}$ [32]. When the smaller the particle size was (18nm), the larger the surface area was, the more catalytic activity sites were, and the higher the catalytic activity was. The mesoporous structure of  $\text{Fe}_3\text{O}_4$ MNPs may be more beneficial to BA and  $\text{H}_2\text{O}_2$  to be attracted to the surface. Furthermore, the modification groups of  $\text{Fe}_3\text{O}_4$ MNPs surface will affect the interaction with  $\text{Fe}_3\text{O}_4$ MNPs and substrates. So the targeted nanoparticles used in this study which were not modified had higher catalytic activity than others[33].

*Table 1. Comparison of various methods for the determination of  $\text{H}_2\text{O}_2$  with different sensors.*

Methods	Materials	Linear range ( $\mu\text{M}$ )	LOD ( $\mu\text{M}$ )	References
electrochemistry	Nanoporous silver/Ni wire	10~8000	4.8	[15]
spectrophotometry	Ionic liquid coated iron nanoparticles	30~300	0.15	[6]
spectrophotometry	$\text{Fe}_3\text{O}_4$ NP/montmorillonite	50~200	5.1	[33]
chemiluminescence	MOF-235/ $\beta$ -cyclodextrin	0.01~1	0.005	[14]
fluorospectrophotometry	m-NBBB and p-NBBB	1.0~100	0.16	[12]
fluorospectrophotometry	$\text{MoS}_2$ nanosheets	5.5~12.6	0.50	[20]
fluorospectrophotometry	polydopamine-glutathione nanoparticles	0.5~6	0.15	[21]
Our method	$\text{Fe}_3\text{O}_4$ MNPs	0.5~12.5	0.122	this work

### 3.5. Repeatability, reproducibility and stability analysis

The repeatability of the  $\text{Fe}_3\text{O}_4/\text{H}_2\text{O}_2/\text{BA}$  fluorescence system was examined by hydrogen peroxide detection ( $10\mu\text{M}$ ) for five successive determinations with a relative standard deviation (RSD) of 3.05%, indicating a good repeatability of the system. The inter-assay precision was estimated at five different  $\text{Fe}_3\text{O}_4/\text{H}_2\text{O}_2/\text{BA}$  fluorescence system using  $10\mu\text{M}$  hydrogen peroxide with 9.09% RSD. As it is more easily oxidized, the  $\text{Fe}_3\text{O}_4$ MNPs cannot preserve in extended dry conditions and hence must be stored in alcohol at  $4^\circ\text{C}$ . In stability tests, it was noted that after a span of 15 days, the signal strength decreased a maximum by  $17.45\pm 0.57\%$ . It can be deduced from these data that under optimized conditions and proper storage environment, the detection shows acceptable repeatability, reproducibility and stability.

### 3.6. Selectivity and interference analysis

We further examined the specificity of the  $\text{Fe}_3\text{O}_4/\text{H}_2\text{O}_2/\text{BA}$  fluorescence system toward  $\text{H}_2\text{O}_2$  detection, and the experiments were performed under the same conditions using interferences such as  $\text{K}^+$ ,  $\text{Na}^+$ ,  $\text{Mg}^{2+}$ ,  $\text{Cl}^-$ ,  $\text{SO}_4^{2-}$  and  $\text{Ca}^{2+}$  ( $4.0\text{mM}$ ). To determine the

discrimination ability of this method, fluorescence intensity ( $F-F_0$ ) was determined on various samples. The effect of interferences on the determination of hydrogen peroxide ( $2.0\mu\text{M}$ ) was shown in Figure 6. As shown in Figure 6, this system is highly sensitive and selective toward  $\text{H}_2\text{O}_2$  which the relative standard deviation (RSD) of samples was 4.86% ( $n=6$ ) by origin 8.0. As a result, high specificity is guaranteed in this system.

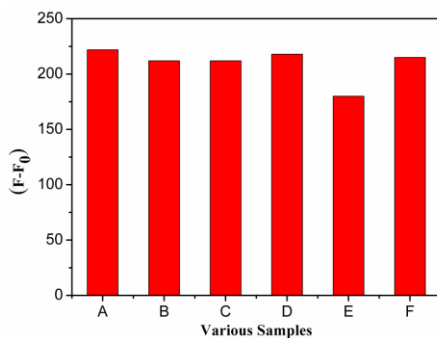


Fig. 6. The effect of interfering substances on catalytic activity of  $\text{Fe}_3\text{O}_4\text{MNPs}$ : A. Sample ( $2\mu\text{M}$ ); B. Sample ( $+4\text{mmolL K}^+$ ); C. Sample ( $+4\text{mmolL Cl}^-$ ); D. Sample ( $+4\text{mmolL Na}^+$ ); E. Sample ( $+4\text{mmolL Mg}^{2+}$ ); F. Sample ( $+4\text{mmolL Ca}^{2+}$ ).

### 3.7. Determination of $\text{H}_2\text{O}_2$ in Samples of Disposable Chopsticks

We tested our method in the determination of residual  $\text{H}_2\text{O}_2$  in disposable chopsticks (Table 2). The fluorescence intensities measured on three parallel samples were substituted into the standard curve to calculate the concentration of hydrogen peroxide, which were converted into the residual of hydrogen peroxide of disposable chopsticks. The calculated  $\text{H}_2\text{O}_2$  contents in each sample are listed in Table 2. The average hydrogen peroxide content in disposable chopsticks by three samples was  $2.763\pm 0.106$  mg/kg. The results were listed in Table 2, it can be seen that the data of recovery is between 92.87% and 108.89%. The RSD of detection were range from 1.24% to 4.99%. It can be seen that the fluorescence system for  $\text{H}_2\text{O}_2$  determination has a good repeatability, precision and recovery. According to iodimetry in National Food Safety Standard of China (GB 5009.226-2016), the residual  $\text{H}_2\text{O}_2$  in disposable chopsticks has not been quantitatively detected with the higher detection limit (3.0mg/kg). The residual  $\text{H}_2\text{O}_2$  in disposable chopsticks from three universities in China was inspected for safety. The fluorescence method can be applied to the determination trace  $\text{H}_2\text{O}_2$  of various sample in food and agricultural industry. Samples A of disposable chopsticks were obtained from restaurants of Guangxi University of Science and Technology, in Liuzhou, China. Samples B of disposable chopsticks were obtained from restaurants of Guangxi University, in Nanning, China. Samples C of disposable chopsticks were obtained from restaurants of Guangxi Normal University, in Guilin, China. Results are expressed as mean  $\pm$  SD of triplicate determinations. Means of  $\text{H}_2\text{O}_2$  content which carry different superscript letters are significantly different at  $P \leq 0.05$ .

Table 2. Results of the analysis of H<sub>2</sub>O<sub>2</sub> in Disposable Chopsticks.

Samples	Manufacture factory	Batch number	Added (μM)	Detected (μM)	Recovery (% , n=3)	RSD (%)	H <sub>2</sub> O <sub>2</sub> content (mg/Kg)
A	Nvhuan Toothpick factory	2017.9.18	0	1.312±0.055 <sup>a</sup>	–	4.19	2.716±0.11
A1			0.5	1.791±0.065 <sup>c</sup>	92.87	3.78	
A2			1.0	2.406±0.060 <sup>b</sup>	105.80	2.49	
A3			2.0	3.335±0.081 <sup>a</sup>	102.57	2.43	
B	Qingying Commodity Co.Ltd.	2017.6.20	0	0.917±0.021 <sup>a</sup>	–	2.29	1.993±0.04
B1			0.5	1.481±0.074 <sup>b</sup>	102.17	4.99	
B2			1.0	2.110±0.091 <sup>c</sup>	95.67	4.31	
B3			2.0	3.199±0.101 <sup>a</sup>	101.00	3.15	
C	Kangjie bamboo products factory	2017.10.19	0	1.187±0.029 <sup>a</sup>	–	2.44	2.255±0.06
C1			0.5	1.799±0.076 <sup>c</sup>	94.88	4.22	
C2			1.0	2.206±0.066 <sup>b</sup>	106.89	2.99	
C3			2.0	3.300±0.041 <sup>a</sup>	98.87	1.24	
Average							2.321±0.32

Samples A of disposable chopsticks were obtained from restaurants of Guangxi University of Science and Technology, in Liuzhou, China. Samples B of disposable chopsticks were obtained from restaurants of Guangxi University, in Nanning, China. Samples C of disposable chopsticks were obtained from restaurants of Guangxi Normal University, in Guilin, China. Results are expressed as mean ± SD of triplicate determinations. Means of H<sub>2</sub>O<sub>2</sub> content which carry different superscript letters are significantly different at  $P \leq 0.05$ .

#### 4. Conclusions

In this study, a simple and sensitive H<sub>2</sub>O<sub>2</sub>-involved fluorescence system with low detection limit was developed using Fe<sub>3</sub>O<sub>4</sub>MNPs as peroxidase mimetic enzyme and benzoic acid (BA) as indicator. The Fe<sub>3</sub>O<sub>4</sub>MNPs were used as mimetic enzyme, resulted in higher magnetic separation (<10 s) and the small sized sample volume (50 μL). The method is highly selective over several potentially interfering ions and agents. Under the optimal reaction conditions, the determination of the residue H<sub>2</sub>O<sub>2</sub> in disposable chopsticks was 2.321±0.32 mg/kg with the RSD of detection were range from 1.24% to 4.99%. The fluorescence spectrometry method by using Fe<sub>3</sub>O<sub>4</sub>MNPs as mimetic enzyme has a good repeatability, precision and recovery which could be used to detect trace H<sub>2</sub>O<sub>2</sub> of various samples. We believe that the method for H<sub>2</sub>O<sub>2</sub> determination described here would be of great value in food and agricultural industry.

## Acknowledgements

This work was supported by the National Natural Science Foundation of China (2176600) and Natural Science Foundation of Guangxi Province (2019GXNSFBA245098).

## References

- [1] C. Chao, T. Qian, L. Qi, *Food Research and Development* **39**(12), 220 (2018).
- [2] C. P. Lu, C. T. Lin, C. M. Chang, S. H. Wu et al., *J. Agric. Food Chem.* **59**(21), 11403 (2011).
- [3] S. C. Su, C. H. Liu, H. C. Chen et al., *Journal of Food & Drug Analysis* **7**(2), 131(1999).
- [4] C. X. Wang, *Advanced Measurement and Laboratory Management* **18**(04), 13(2010).
- [5] S. C. Sui, S. S. Chou, P. C. Chang et al., *Journal of Food & Drug Analysis* **9**(4), 220 (2001).
- [6] F. Zarif, S. Rauf, M. Z. Qureshi, N. S. Shah et al., *Microchimica Acta* **185**(6), 302 (2018).
- [7] T. G. Choleva, V. A. Gatselou, G. Z. Tsogas et al., *Mikrochimica Acta* **185**(1), 22 (2018).
- [8] Y. Ding, M. Chen, K. Wu et al., *Materials Science & Engineering C* **80**, 558 (2017).
- [9] J. Pang, Y. Zhao, H. L. Liu et al., *Talanta* **185**, 581 (2018).
- [10] T. Rui, Z. Boyu, Z. Mingming et al., *Talanta* **188**, 332 (2018).
- [11] J. Chen, Y. Gao, Q. Ma et al., *Sensors & Actuators B Chemical* **268**, 270 (2018).
- [12] B. S. Li, J. Chen, Y. Xiong et al., *Sensors and Actuators B* **268**, 475 (2018).
- [13] D. X. Kong, S. Huang, J. Cheng et al., *Luminescence* **33**(4), 698 (2018).
- [14] X. Mao, Y. Lu, X. Zhang et al., *Talanta* **188**, 161 (2018).
- [15] X. L. Zou, Y. He, P. Sun, J. Zhao et al., *Applied Surface Science* **447**, 542 (2018).
- [16] L. Y. Wang, M. Xu, Y. Xie, Y. Song et al., *Journal of Materials Science* **53**(15), 10946 (2018).
- [17] Y. Gao, G. N. Wang, H. Huang et al., *Talanta* **85**, 1075 (2011).
- [18] Q. Chang, H. Tang, *Microchimica Acta* **181**(5-6), 527 (2014).
- [19] X. Xu, L. Song, Q. Zheng et al., *Electroanalysis* **29**(3), 765 (2016).
- [20] H. M. Liu, B. Wang, D. Li, X. Zeng et al., *Microchimica Acta* **185**(6), 287(2018).
- [21] L. Tang, S. Mo et al., *Sensors and Actuators B* **259**, 467 (2018).
- [22] W. Luo, Y. S. Li, J. Yuan et al., *Talanta* **81**(3), 901 (2010).
- [23] Y. Shi, P. Su, Y. Wang et al., *Talanta* **130**, 259 (2014).
- [24] S. Hashemian, H. Saffari, *Asian Journal of Chemistry* **23**(6), 2815 (2011).
- [25] A. Dandia, V. Parewa, S. L. Gupta et al., *Catalysis Communications* **61**, 88 (2015).
- [26] J. Dong, L. Song, J. J. Yin et al., **6**(3), 1959 (2014).
- [27] Z. W. Chen, J. J. Yin, Y. T. Zhou et al., *ACS Nano* **6**(5), 4001 (2012).
- [28] A. Hiroki, J. A. Laverne, *The Journal of Physical Chemistry B* **109**(8), 3364 (2005).
- [29] J. Mu, L. Zhang, M. Zhao et al., *Journal of Molecular Catalysis A: Chemical* **378**, 30 (2013).
- [30] J. Dong, L. Song, J. J. Yin et al., *Acs Applied Materials & Interfaces* **6**(3), 1959 (2014).
- [31] R. Reske, H. Mistry, F. Behafarid et al. *Journal of the American Chemical Society* **136**(19), 6978 (2014).
- [32] L. Gao, J. Zhuang, L. Nie et al., *Nature Nanotechnology* **2**(9), 577 (2007).
- [33] K. Wu, X. Zhao, M. Chen et al., *New Journal of Chemistry* **42**(12), 9578 (2018).